N-methyl-d-aspartate receptor independent changes in expression of polysialic acid-neural cell adhesion molecule despite blockade of homosynaptic long-term potentiation and heterosynaptic long-term depression in the awake freely behaving rat dentate gyrus

Journal Item

Neuron Glia Biology, page 1 of 10.
doi:10.1017/S1740925X09990159

N-methyl-D-aspartate receptor independent changes in expression of polysialic acid-neural cell adhesion molecule despite blockade of homosynaptic long-term potentiation and heterosynaptic long-term depression in the awake freely behaving rat dentate gyrus

J. J. RODRÍGUEZ[1,2*], G. M. DALLÉRAC[3*], M. TABUCHI[1], H. A. DAVIES[4], F. M. COLYER[4], M. G. STEWART[4] AND V. DOYÈRE[3]

Investigations examining the role of polysialic acid (PSA) on the neural cell adhesion molecule (NCAM) in synaptic plasticity have yielded inconsistent data. Here, we addressed this issue by determining whether homosynaptic long-term potentiation (LTP) and heterosynaptic long-term depression (LTD) induce changes in the distribution of PSA-NCAM in the dentate gyrus (DG) of rats in vivo. In addition, we also examined whether the observed modifications were initiated via the activation of N-*methyl-*D-*aspartate (NMDA) receptors. Immunocytochemical analysis showed an increase in PSA-NCAM positive cells both at 2 and 24 h following high-frequency stimulation of either medial or lateral perforant paths, leading to homosynaptic LTP and heterosynaptic LTD, respectively, in the medial molecular layer of the DG. Analysis of sub-cellular distribution of PSA-NCAM by electron microscopy showed decreased PSA dendritic labelling in LTD rats and a sub-cellular relocation towards the spines in LTP rats. Importantly, these modifications were found to be independent of the activation of NMDA receptors. Our findings suggest that strong activation of the granule cells up-regulates PSA-NCAM synthesis which then incorporates into activated synapses, representing NMDA-independent plastic processes that act synergistically on LTP/LTD mechanisms without participating in their expression.*

Keywords: Adhesion molecules, hippocampus, synaptic plasticity

INTRODUCTION

Synaptic morphological changes occur following induction of synaptic plasticity with high-frequency electrical stimulation or after behavioural learning (Eyre *et al.*, 2003; Stewart *et al.*, 2005; Miranda *et al.*, 2006; Platano *et al.*, 2008). Neural cell adhesion molecules (NCAMs) may participate in these changes as they control adhesion forces between cellular membranes and therefore, indirectly, synaptic stability (see Gascon *et al.*, 2007 for a recent review). NCAMs, which are glycoproteins of the immunoglobulin superfamily, have traditionally been implicated in developmental processes such as the maturation and migration of newly formed neurons (reviewed in Rutishauser, 2008). In the past decade, a growing body of evidence has shown that NCAMs play also an important role in cognitive and plastic processes at the synapse in adulthood (Arami *et al.*, 1996; Roullet *et al.*, 1997; Mileusnic *et al.*, 1999; Foley *et al.*, 2003; Stoenica *et al.*, 2006). NCAM function can be up- and down-regulated through post-translational modifications (Schachner, 1997; Kiss and Muller, 2001). Polysialic acid (PSA) is a long negatively charged carbohydrate that has so far only been found on NCAM molecules in the mammals. PSA is attached by the polysialyltransferases PST and STX on the homophilic interaction sites of the molecules and thereby reduces NCAM–NCAM trans- and cis interactions, thus decreasing their function (Rutishauser and Landmesser, 1996). Therefore, the addition of long chains of PSA to NCAM modifies the relative degree of overall membrane apposition between cells, a mechanism that is involved in neural plasticity (Rougon, 1993; Seki and Arai, 1993).

Polysialylation of NCAMs has been implicated in hippocampus-dependent memory storage (Fox *et al.*, 1995; Foley *et al.*, 2003; Florian *et al.*, 2006; Venero *et al.*, 2006; Lopez-Fernandez *et al.*, 2007; Markram *et al.*, 2007). Long-term potentiation (LTP) and long-term depression (LTD) are widely accepted models of plasticity involved in memory processes. However, to date, the role of PSA-NCAM in the dentate gyrus (DG) synaptic plasticity remains largely unknown. Indeed, whereas LTP and LTD in the CA1 area of the hippocampus have been shown to be impaired *in vitro* after specific removal of PSA with the enzyme Endo-N (Becker *et al.*, 1996; Muller *et al.*, 1996) or using knock-out mice (Eckhardt *et al.*, 2000), normal LTP was found *in vivo* in the DG of transgenic mice lacking

Corresponding authors:
V. Doyère and J. J. Rodríguez
Emails: valerie.doyere@u-psud.fr; Jose.Rodriguez-arellano@manchester.ac.uk
*Equally contributed.

either PST or STX (Stoenica *et al.*, 2006). Whether the discrepancies originate from the *in vitro*/*in vivo* preparation difference or CA1/DG region specificity is unclear. It remains possible that the activity of the remaining polysialyltransferase in knock-out animals is sufficient to maintain an appropriate level of PSA-NCAM during synaptic plasticity in the DG. Alternatively, polysialization of NCAM may simply not be implicated in LTP in the DG.

OBJECTIVES

Whereas behavioural studies have found increases in PSA-NCAM in the DG after training (Fox *et al.*, 1995; Foley *et al.*, 2003; Venero *et al.*, 2006; Lopez-Fernandez *et al.*, 2007), no study to date has examined whether LTP or LTD would also produce changes in PSA-NCAM in the DG. Therefore, we sought to examine this issue *in vivo* in the awake rat. We took advantage of the fact that both homosynaptic LTP and heterosynatpic LTD can be induced *in vivo* in the middle molecular layer of the DG with a comparable level of cellular activation; i.e. high-frequency stimulation (HFS) of the medial or lateral perforant path (LPP), respectively. Both immunocytochemistry and electron microscopy (EM) analyses were used in order to determine whether homosynaptic LTP and heterosynaptic LTD induce specific changes in the magnitude and distribution of PSA-NCAM in the DG, as well as more subtle alterations in its sub-cellular localization. Importantly, we also tested whether these changes were initiated, as LTP and LTD, through the activation of *N*-methyl-D-asparate (NMDA) receptors.

MATERIALS AND METHODS

Surgical procedures

All animal experimental procedures were carried out at Neurobiologie de l'Apprentissage, de la Mémoire et de la Communication, CNRS-Université Paris-Sud, in accordance with guidelines of the EU, CNRS and the French Agricultural and Forestry Ministry (decree 87848; licence no. A91429). Subjects were adult male Sprague–Dawley rats (Charles River, France) weighing 300–350 g and housed individually with food and water *ad libitum* in a temperature-controlled room and on a 12 h light/dark cycle. Experiments were conducted within the 12 h light phase. Thirty-one animals were anaesthetized with sodium pentobarbitone (60 mg·kg^{-1}, i.p.) and prepared for chronic recording as described previously (Doyere *et al.*, 1997; Mezey *et al.*, 2004). Briefly, animals were placed on a stereotaxic apparatus and kept at a constant temperature of 37°C. The recording electrode consisted in two 65-μm nichrome recording wires extending 1.5 mm from a stainless steel microtube and was implanted in the hilus of the left DG (AP 4.2 mm; L 2.5 mm from Bregma). Two concentric bipolar electrodes were, respectively, placed in the lateral perforant path (LPP coordinates: AP 8.2 mm, L 4.8 ± 5.2 mm from Bregma) and medial perforant path (MPP coordinates: AP 7.8 mm, L 4.2 mm from Bregma). All electrodes were positioned at the optimal depth to maximize the slope of the positive-going field excitatory post-synaptic potential (EPSP) evoked by stimulation of each pathway. The microtube was used as reference electrode and the ground was connected to a silver ball placed under the skull. All electrodes were connected to multichannel miniature sockets, fixed to the skull with dental acrylic. Rats were treated with antibiotic (Terramycin, 20 mg·kg^{-1}, i.p.) for 5 days and were allowed to recover a minimum of 10 days.

Electrophysiology and experimental design

All electrophysiological data were obtained in awake rats and experimental procedures were similar to those previously reported (Mezey *et al.*, 2004). In short, after 3 days of habituation to the recording chamber (30 min each day) during which input/output curves and convergence and summation tests were carried out, a pre-HFS baseline was recorded by stimulating alternately the two pathways at 15 s intervals for 20 min using test intensities (mean 400 μA, 80–120 μs) to evoke MPP and LPP EPSP slopes of approximately half its maximum. The latency and shape of the field potentials (with the spike on the ascending phase of EPSP for the medial path, and on the descending phase of EPSP for the lateral path, both before and after HFS (Abraham and McNaughton, 1984), were also criteria for assessing pathway selectivity. On the day of LTP induction, after a 20 min baseline, HFS was delivered, and recordings were resumed for 30 min. A post-HFS baseline was finally recorded either 2 or 24 h later immediately before the perfusion of the animals. Hippocampal EEG was continuously monitored during recording sessions to ensure the absence of electrically induced afterdischarges.

Seven animal groups were considered in this investigation:

2 h LTP group: LTP was induced at MPP synapses terminating in the medial molecular layer (MML) of the DG using a strong tetanization protocol (HFS of ten series of seven 400-Hz trains, 20 ms duration (eight pulses), 1 s intertrain interval, 1 min between each series) applied at test intensity. Rats were perfused immediately after the baseline recorded 2 h after HFS.

24 h LTP group: LTP was induced by stimulation of the MPP as described above and the animals were perfused immediately after the baseline recorded 24 h following HFS.

CPP-MPP group: Blockade of homosynaptic LTP by NMDA antagonist – rats received an injection (10 mg·kg^{-1}, i.p.) of the NMDA-receptor antagonist D, L-3[(±)-2-carboxypiperazin-4-yl] – propyl-1-phosphonic acid (CPP, Sigma) 2 h 30 min before baseline recording and therefore 3 h before delivering HFS to the MPP and were perfused at 24 h.

2 h LTD group: Heterosynaptic LTD was induced at MPP synapses using the same strong tetanization protocol but applied to the LPP at test intensity. Rats were perfused immediately after the baseline recorded 2 h after HFS.

24 h LTD group: Heterosynaptic LTD of the MPP was induced by stimulation of the LPP as described for the 2 h LTD group and the animals were perfused immediately after the baseline recorded 24 h following HFS.

CPP-LPP group: Rats received an injection (10 mg·kg^{-1}, i.p.) of CPP 2 h 30 min before baseline recording and therefore 3 h before HFS of the LPP and were perfused at 24 h.

Control group: Rats were either implanted but received no stimulation, or only single test stimulations over 4 days, including immediately before the perfusion of the animal.

Tissue preparation

Rats were deeply anaesthetized with sodium pentobarbital (100 mg·kg^{-1}, i.p.). The brains of these animals were fixed by aortic arch perfusion with 50 ml of 3.8% acrolein (Fluka, UK) in a solution of 2% paraformaldehyde and 0.1 M phosphate buffer (PB), pH 7.4, followed by 250 ml of 2% paraformaldehyde. The brains were removed from the cranium and cut into 4–5 mm coronal slabs of tissue containing the entire rostrocaudal extent of the hippocampus. This tissue was then post-fixed for 30 min in 2% paraformaldehyde and sectioned at 40–50 μm on a VT1000, vibrating microtome (Leica, Milton Keynes, UK). Coronal sections, of the dorsal hippocampus, were selected from each rat at a level −2.40 mm/−4.20 mm posterior to Bregma, according to the rat brain atlas of Paxinos and Watson (1998), at least 100 μm from the electrode tractus. To remove excess reactive aldehydes, sections were treated with 1% sodium borohydride in 0.1 M PB for 30 min. The sections were then rinsed with 0.1 M PB followed by 0.1 M Tris-buffered saline (TBS), pH 7.6.

Immunocytochemistry

To optimize detection of PSA-NCAM containing cells and profiles the sections of all animals were processed using the avidin–biotin peroxidase complex (ABC) method (Hsu *et al.*, 1981). For this procedure, vibrating microtome sections were first incubated for 30 min in 0.5% bovine serum albumin in TBS to minimize non-specific labelling. The tissue sections were then incubated for 48 h at room temperature in 0.1% bovine serum albumin in TBS containing 0.25% Triton X-100 and mouse monoclonal antibody against PSA-NCAM (AbC0019, Abcys SA, Paris, France) at a dilution of 1:250. Sections were then washed and placed in (1) 1:200 dilution of biotinylated donkey anti-mouse immunoglobulin (IgM, Jackson ImmunoResearch, West Grove, PA, USA) and (2) 1:200 dilution of biotin–avidin complex from the Elite kit (Vector Laboratories Ltd., Peterborough, UK) for 1 h each. All antisera dilutions were prepared in 0.1% BSA in TBS, and the incubations were carried out at room temperature. The peroxidase reaction product was visualized by incubation in a solution containing 0.022% of 3,3-diaminobenzidine (DAB, Aldrich, Gillingham, UK) and 0.003% H_2O_2 in TBS for 7 min. The sections were then permanently mounted on gelatin-coated glass slides and coverslipped with Entellan (Merck, Darmstadt, Germany) mounting medium. Specificity of PSA-NCAM antiserum was checked by incubating the sections with (i) normal serum instead of primary antibody, or (ii) normal serum instead of the secondary biotinylated antibody. No immunostaining was seen on any of these sections.

For EM pre-embedding immunogold-silver labelling (Chan *et al.*, 1990), sections were rinsed in 0.01 M phosphate-buffered saline pH 7.4 (PBS), and blocked in 0.8% BSA and 0.1% coldwater fish gelatin in PBS (BSA/gelatin) for 10 min and incubated in the primary antibody at a dilution of 1:50 under the same conditions as for light immunocytochemistry. Following this incubation, sections were processed for 2 h in a 1:50 dilution of rabbit anti-goat IgM conjugated with 1 nm colloidal gold (British Biocell International, Cardiff, UK) in BSA/gelatin, and then rinsed in BSA/gelatin followed by PBS. The bound gold particles were secured in the tissue by placing the sections in 2% glutaraldehyde in 0.01 M PBS for 10 min. These sections were then washed in 0.2 M citrate buffer, and reacted for 6–8 min with a silver enhancement solution (British Biocell International, Cardiff, UK). The silver reaction was stopped by successive rinses in citrate buffer.

Electron microscopic examination, nomenclature and analysis

For EM, ultrathin sections were cut and collected on pioloform/carbon filmed copper slot grids. These sections were counterstained with uranyl acetate and lead citrate (Reynolds, 1963) and examined in either a JEOL-1010 or JEOL-1400 electron microscope equipped with an AMT XR40 or XR60 digital camera, respectively. Labelled profiles were classified as dendrites, dendritic spines (not included in the dendritic count) or presynaptic boutons, according to their morphological features as defined by Peters *et al.* (1991). Analysis was exclusively carried out on the most superficial portions of the tissue in contact with the embedding plastic to minimize artificial differences in labelling attributed to potential differences in penetration of reagents (Pickel *et al.*, 1992). Regions chosen for this analysis were based on the presence of PSA-NCAM immunoreactivity and the morphological integrity of the tissue. The labelled profiles were assessed from three coronal vibrating microtome sections of three animals per group in the MML of the DG. Adobe Photoshop and Illustrator (versions 7.0; Adobe Systems) software were utilized to build and label the composite illustrations.

Data analysis

All data are shown with standard error of the mean (SEM). The area density (Sv, number/mm^2) of PSA-NCAM-immunoreactive neurons was expressed as the number of labelled neurons per unit area of section analysed. For light microscopy, the labelled cells were quantified per mm^2 on the ipsilateral DG in three non-consecutive coronal vibrating microtome sections, separated by at least 80 μm, taken through representative sections of the dorsal DG of the hippocampus. The number of PSA-NCAM positive cells and the area measurements were determined in a blind manner. For EM, the area density (Sv) of PSA-NCAM labelled dendrites, spines and presynaptic boutons was expressed per 1000 μm^2 of the area of section analysed. The sub-cellular localization was calculated from the total number of gold particles in the area analysed, differentially expressed as a percentage localized to the membrane compartment in the profiles. Analysis of variance (ANOVA) tests were used to examine differences between the different groups followed by a contrast comparison, using the program VAR3. Adobe Photoshop and Illustrator (versions 7.0; Adobe Systems) software were utilized to build and label the composite illustrations.

RESULTS

Electrophysiology

We produced four experimental groups in which HFS was administered: (1) in the MPP, (2) in the LPP, (3) in the

MPP in the presence of CPP and (4) in the LPP in the presence of CPP. The control group received only baseline stimulations. The homosynaptic LTP induced in the MPP with a magnitude of 31.77 ± 3.56% change ($n = 10$) 30 min post-HFS was maintained 2 h (magnitude: 38.41 ± 7.6% change; $n = 5$; Fig. 1) and 24 h after induction (magnitude: 22.20 ± 2.40% change; $n = 5$; Fig. 1) and was blocked by the presence of the NMDA receptor antagonist CPP immediately (magnitude at 30 min −2.64 ± 4.06% change; significant difference with LTP groups, $F_{1,11} = 30.8$, $P < 0.001$) and for 24 h (6.62 ± 2.83% change, $n = 4$). As described in our previous investigations (Doyere *et al.*, 1997; Mezey *et al.*, 2004), potentiation of the LPP (21.73 ± 8.30% change at 2 h, $n = 5$; 39.80 ± 8.60% change at 24 h, $n = 4$; data not shown) resulted immediately in heterosynaptic LTD of the MPP with a magnitude of −20.57 ± 3.30% change ($n = 9$) 30 min post-HFS, which was maintained at 2 h (−14.30 ± 3.69% change) and at 24 h (−10.36 ± 1.56% change at 24 h; Fig. 1). As shown in Fig. 1C, this heterosynaptic LTD was clearly blocked by CPP immediately after the tetanus (magnitude at 30 min −4.10 ± 3.84% change; significant difference with LTD groups, $F_{1,10} = 9.78$, $P = 0.01$) and for 24 h (−4.18 ± 6.82% change, $n = 4$).

PSA-NCAM expression

In all groups, stimulated and not stimulated at high frequency, it was possible to see PSA-NCAM immunoreactivity (PSA-NCAM-IR) throughout the hippocampus and more specifically within the granule cell layer of the DG (Fig. 2A,B). PSA-NCAM-IR cells were localized mainly in the basal layers of the DG and displayed all the characteristics of granule cells, with a round/ovoid somata radiating multiple dendrites into the different subdivisions of the molecular layer (Figs 2A,B and 3B). This dendritic arborization gave rise to a complex network that extended from the inner molecular layer, where it was possible to observe the proximal dendrites, to the middle and outer molecular layers where some thinner processes, possibly dendritic spines, could be observed and could be identified further by EM (Figs 2A,B and 4A,B). Following HFS of the MPP we could observe a significant increase in the area density of PSA-NCAM positive cells ($F_{1,14} = 9.65$, $P < 0.01$) not only after 2 h but also at 24 h (Control: 245.9 ± 43.18 cells/mm², $n = 4$; 2 h: 396.8 ± 49.79 cells/mm², $n = 5$; 24 h: 395.11 ± 34.91 cells/mm², $n = 5$; Fig. 2). Furthermore, this increase was not

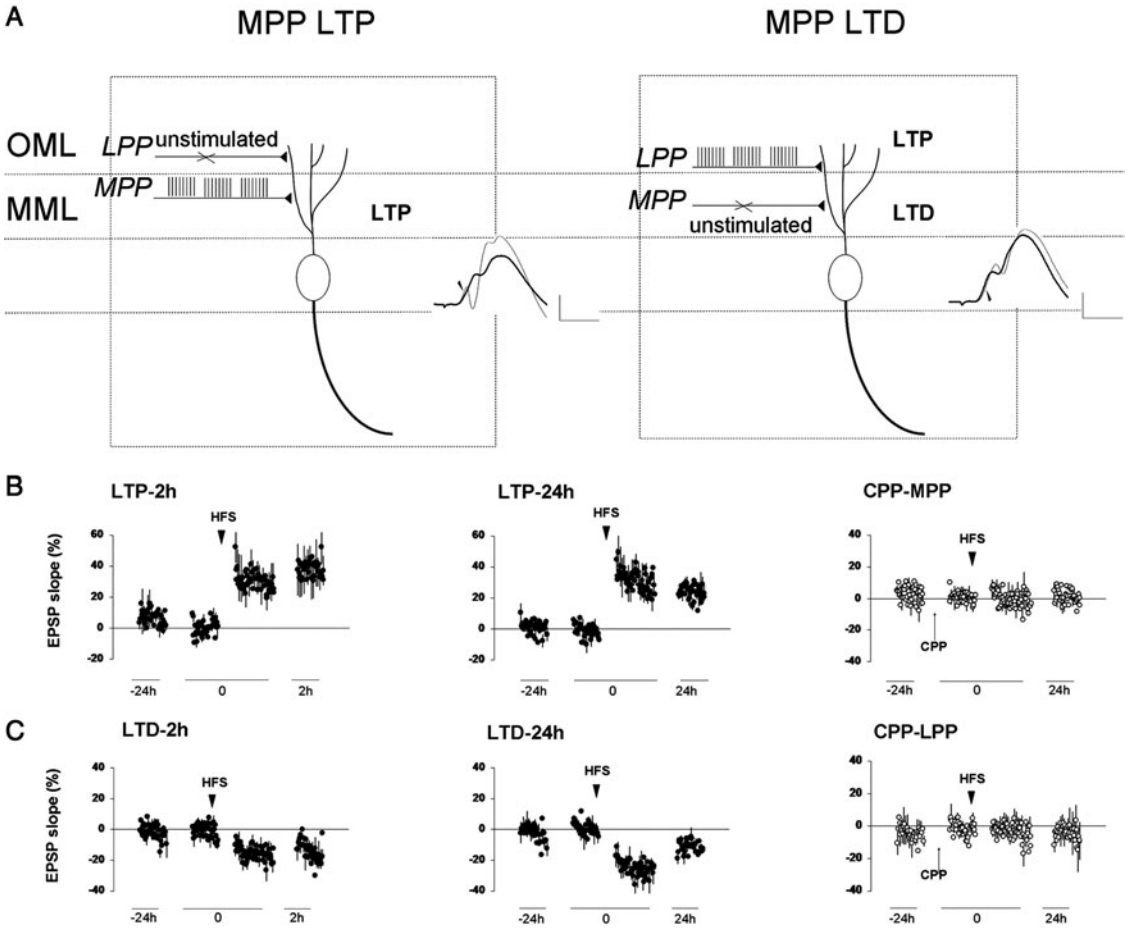

Fig. 1. (A) **Homosynaptic long-term potentiation (LTP) in MML (as observed on the field potential evoked by MPP stimulation) was induced by high-frequency stimulation (HFS) of the MPP while the LPP was unstimulated (left).** Heterosynaptic long-term depression (LTD) in MML was obtained by applying the HFS to the LPP while no stimulation was delivered to the MPP (right). (B) Timeline graphs showing induction of LTP in the MML, as an immediate increase in EPSP slope (% change from baseline) of the field potential evoked by the MPP stimulation, LTP that lasts for 2 and 24 h after HFS delivered the MPP, and is blocked by CPP. (C) Timeline graphs showing induction of heterosynaptic LTD in the MML, as an immediate decrease in EPSP slope (% change from baseline) of the potential evoked by the MPP stimulation, heterosynaptic LTD that lasts for 2 and 24 h after HFS delivered to the LPP, and is blocked by CPP. LPP: lateral perforant path, MML: medial molecular layer, MPP: medial perfotant path, OML: outer molecular layer.

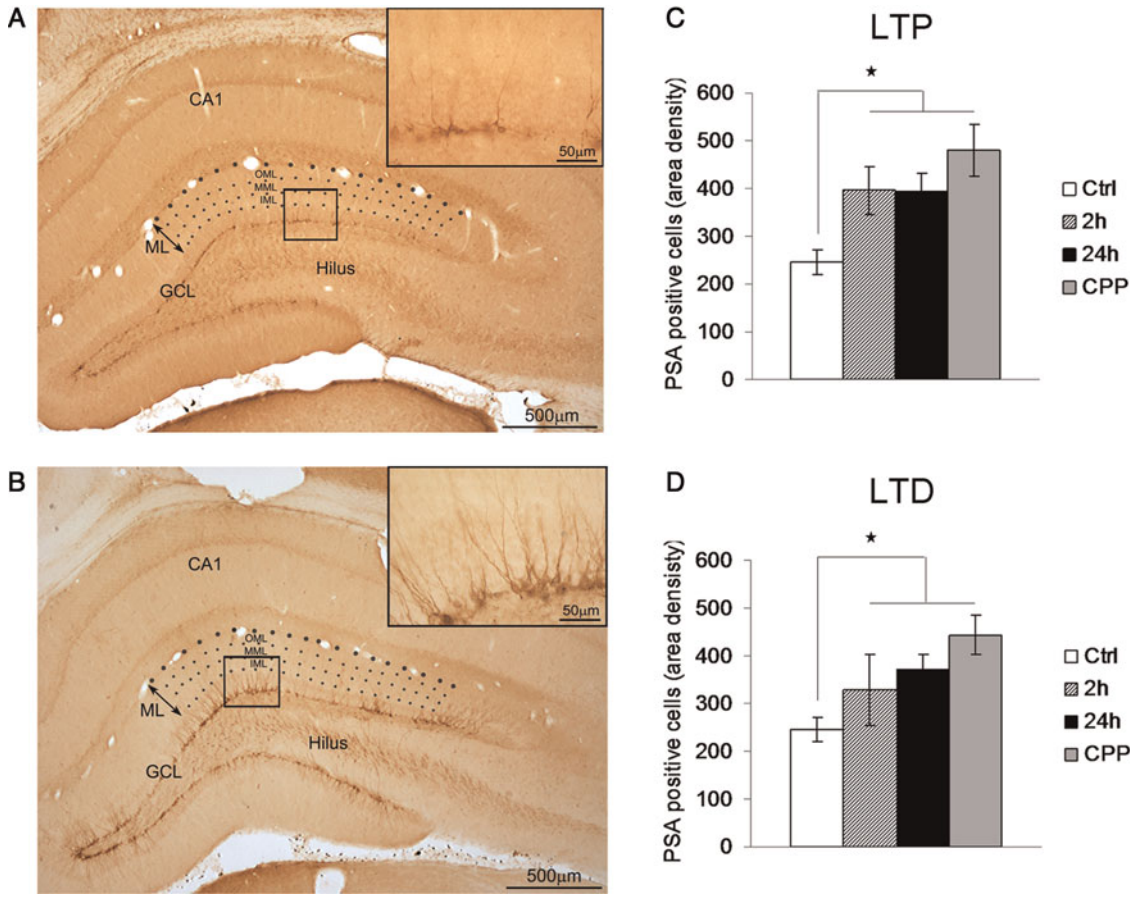

Fig. 2. Polysialic acid-neural cell adhesion molecule (PSA-NCAM positive cells could be detected by immunocytochemistry both in control (A) and high-frequency stimulation (HFS) stimulated (B) groups. Note that there is a remarkable increase in the number of PSA-NCAM positive granule cells and dendritic arborization which was present at 2 h following HFS in the medial perforant path (MPP) (C) ($F_{1,14} = 9.65$, $P < 0.01$) and 24 h following HFS in lateral perforant path (LPP) (D) ($F_{1,13} = 4.9$, $P = 0.04$).

blocked by the administration of the NMDA antagonist, CPP (479.19 ± 54.05 cells/mm^2, $n = 4$; Fig. 2).

After HFS in the LPP we also observed a smaller, but significant increase in the area density of PSA-NCAM-IR cells ($F_{1,13} = 4.9$, $P = 0.04$), which was not blocked by CPP (2 h: 328.53 ± 73.49 cells/mm^2, $n = 5$, 24 h: 372.18 ± 31.68 cells/mm^2, $n = 4$, CPP: 443.73 ± 41.13 cells/mm^2, $n = 4$; Fig. 2).

PSA-NCAM sub-cellular distribution

In order to analyse the sub-cellular localization of PSA moieties in the different stimulation paradigms, we chose to analyse the MML by EM to quantify the specific localization of PSA-NCAM within the different neuronal profiles (dendrites, spines and boutons, $n = 3$ animals in each group) by using an immunogold labelling approach (Figs 3B and 4B). Furthermore, we also were able to compare the proportion of PSA-NCAM present in the plasma membrane versus the cytoplasmic compartment.

HFS applied to the MPP did not significantly affect the area density of PSA-NCAM-IR dendrites (Fig. 3) or the sub-cellular distribution (membrane versus cytoplasm, see Supplementary Fig. 5 online) of PSA positive dendrites. In contrast, the number of PSA labelled dendrites decreased after tetanization of the LPP regardless of the perfusion time or the presence of CPP (Control: 38.36 ± 7.5 dendrites/1000 μm^2; 2 h: 16.3 ± 1.6 dendrites/1000 μm^2, 24 h: 25.06 ± 7.33 dendrites/1000 μm^2; 22.83 ± 5.84 dendrites/1000 μm^2; Fig. 3). An analysis by contrast confirmed a significant decrease in the area density of PSA positive dendrites when all groups tetanized via the LPP were compared to the untetanized control ($F_{1,8} = 5.64$, $P = 0.04$; Fig. 3B). This is in agreement with the light microscopy immunocytochemistry where there is an increase in PSA positive cell bodies, that is independent of the NMDA-receptor activation and is not only present at 2 h but persists 24 h post-HFS. Although the compartmental distribution (membrane versus cytoplasm, $F_{>1}$, $P > 0.05$) of dendritic PSA after LPP tetanization was not significantly altered, there was a tendency for changes in the sub-cellular distribution of PSA moieties which were opposite for LTP and LTD and marginally significant at 24 h post-HFS (Control: 26.30 ± 5.54% of membranar PSA moieties, LTP 24 h: 19.79 ± 5.36%, LTD 24 h: 39.63 ± 6.54%; LTP 24 h versus LTD 24 h: $F_{1,4} = 5.50$, $P = 0.08$; see Supplementary Fig. 5 online).

The area density of PSA-NCAM labelled spines increased significantly when HFS was applied to the MPP ($F_{1,8} = 5.14$, $P = 0.05$) but not to the LPP despite a clear trend in the CPP group. Such augmentation was observed at 2 and 24 h post-HFS, as well as in the presence of CPP (Control: 0.9 ± spines/1000 μm^2, 2 h: 2.11 ± 0.44 spines/1000 μm^2, 24 h:

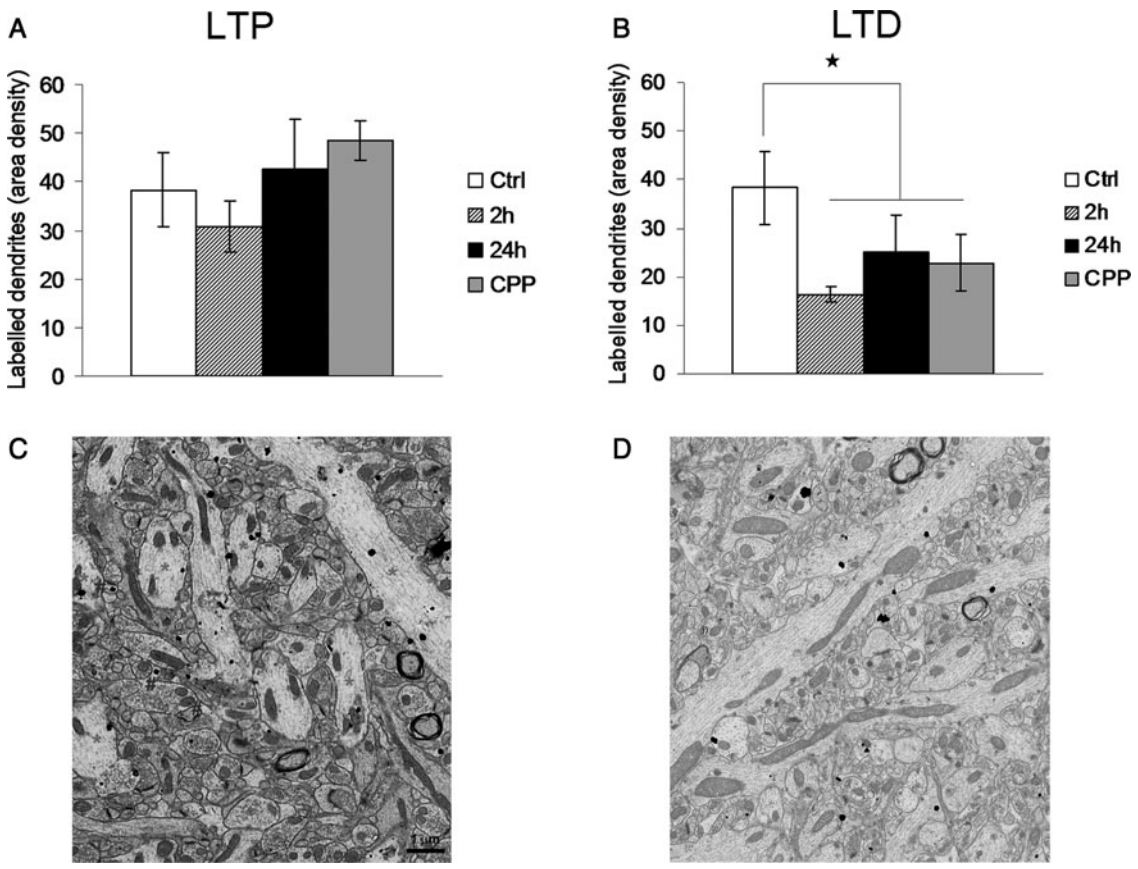

Fig. 3. The area density of labelled dendrites was found unchanged in the homosynaptic long-term potentiation (LTP) group (A). In contrast HFS applied to the lateral perforant path (LPP) induced a decrease in polysialic acid (PSA) positive dendrites at 2 h, 24 h and in the presence of CPP (B; $F_{1,8} = 5.64$, $P = 0.04$). Lower panels: dendrites (red asterisks) and dendritic spines (blue labels) from the medial molecular layer (MML) of the dentate gyrus in control (C) and heterosynaptic long-term depression (LTD) (D) animals containing immunogold labelling for PSA-neural cell adhesion molecule (NCAM). Note that there is a marked decrease in both the number of PSA-NCAM positive dendrites and spines after heterosynaptic LTD.

2.43 ± 0.23 spines/1000 μm^2, CPP: 1.99 ± 0.7 spines/1000 μm^2; Fig. 4). Consequently, the variation in the area density of PSA positive spine appears specific to the MPP tetanization, is already present at 2 h, persists 24 h post-HFS and, once more, is independent of the NMDA-receptor activation. We found no difference in the sub-cellular localisation of PSA molecules within spines (data not shown). No significant change in the area density of labelled boutons was detected, but a marginally significant decrease in membranar PSA moieties (membrane *vs*. cytoplasm) within boutons after tetanization of both the LPP ($F_{1,8} = 3.49$, $P = 0.10$) and MPP ($F_{1,8} = 4.06$, $P = 0.08$) was observed (see Supplementary Fig. 6 online).

CONCLUSIONS

- HFS induce a NMDA-receptor independent increase in PSA-NCAM expression.
- PSA-NCAM is redistributed to stimulated synapses.

DISCUSSION

In this investigation we show that polysialylation of the NCAM molecule is upregulated in the DG following tetanic stimulation delivered to the medial or lateral perforant path *in vivo*. However, we also show here for the first time that such an increase appears to be independent of the expression of homosynaptic LTP or heterosynaptic LTD induced by the tetanization. In effect, PSA-NCAM up-regulation was not blocked by the NMDA-receptor inhibitor CPP, while both LTP and LTD were. This result contrasts with other systems in which activation of NMDA-receptors has been shown to modulate the expression of NCAM (Bouzioukh *et al.*, 2001) as well as PSA-NCAM *in vitro* (Wang *et al.*, 1996; Singh and Kaur, 2007) and *in vivo* (Bouzioukh *et al.*, 2001). While the changes reported on NCAM are inhibited by the use of the NMDA receptor antagonist, MK-801 (Schuster *et al.*, 1998), there is some evidence that NMDA receptors can downregulate the expression of PSA-NCAM as observed by Bouzioukh *et al.* (2001) in adult brain stem synapses. The available data from preparation in DG suggest that the changes observed in NCAM180, the major isoform of NCAM, are directly associated with particular NMDA and AMPA receptors subunits such as NR2A and GluR2/3 (Fux *et al.*, 2003) whereas data obtained in cultured CA1 neurons suggest that PSA-NCAM changes may be associated with NMDA NR2B subunit as well as with the AMPA GluR1 subunit (mainly) (Vaithianathan *et al.*, 2004; Hammond *et al.*, 2006). The data we report herein suggest that different mechanisms may be at play in the DG.

Interestingly, administrations of NMDA-receptor antagonists have been found to enhance neurogenesis and therefore PSA positive cells not only in the rat DG, but also in

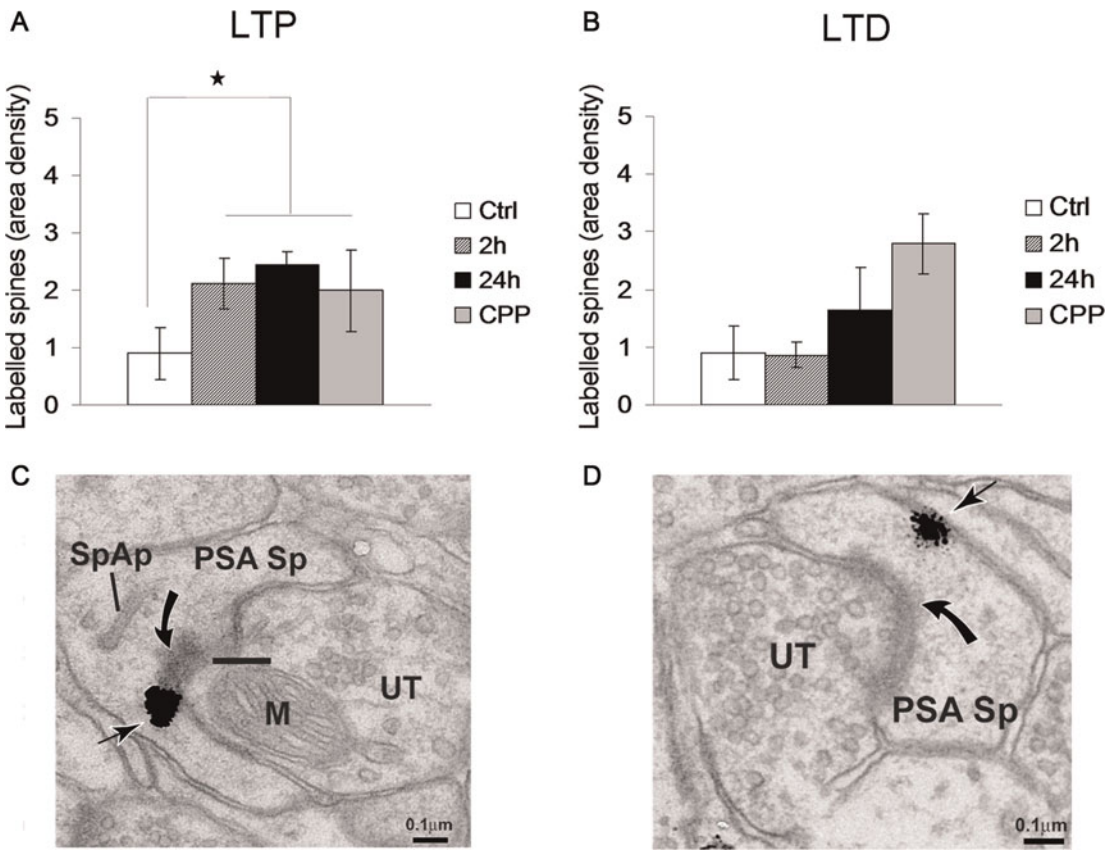

Fig. 4. The area density of labelled spines was increased in the homosynaptic long-term potentiation (LTP) group at 2 h, 24 h and in the presence of CPP (A; $F_{1,8} = 5.14$, $P = 0.05$). No change was detected when heterosynaptic long-term depression (LTD) was induced in the medial molecular layer (MML) (B). On the lower panels (C,D), one can see some examples of polysialic acid-neural cell adhesion molecule (PSA-NCAM) immunogold labelling (straight arrows) in dendritic spines (PSA SP) within the plasma membrane, being in some cases perisynaptic intimately associated with the post-synaptic densities (curved arrows). Both spines are receiving excitatory asymmetric synapses (curved arrows) from unlablled terminals (UT). M: mitochondrion, SpAp: spinous apparatus.

the piriform cortex where neurogenesis does not occur, suggesting that labelling of newborn cells is not the only source of the increase in PSA-NCAM immunopositive neurons (Nacher *et al.*, 2001, 2002). However, the effect reported by Nacher and collaborators was effective only 7 days after administration of the NMDA-receptor antagonist CPG43487 in both structures. In addition, administration of ethanol, another NMDA-receptor antagonist, also results in an increase in neurogenesis 48 h as well as 7 days after intake, but noticeably not 24 h after intake (Nixon *et al.*, 2008). Therefore, although we cannot exclude the hypothesis that the tendency for a higher number of PSA-NCAM immunopositive cells in our study might be the result of the blockade of a downregulation of NCAM polysialylation normally exerted by the activation of NMDA receptors, we believe that it is unlikely given the early time point of perfusion of the animals (27 h following CPP administration). Instead, we favour the hypothesis that a mechanism which is not disturbed by the blockade of NMDA-dependent plasticity, but is still induced by HFS and depolarization would most likely trigger the up-regulation of PSA-NCAM expression in DG cell bodies. The expression of PSA is regulated by the polysialyltransferase PST and STX mainly at the transcription level but also in post-translational ways (reviewed in Angata and Fukuda, 2003). Since the transcription of at least one of the polysialyltransferases (STX) has been shown to be activated by the cAMP response element binding protein (CREB) (Nakagawa *et al.*, 2002) and that CREB is activated by calcium entry through both NMDA-receptors and L-type voltage-dependent calcium channels (VDCC) (Sheng *et al.*, 1991; Deisseroth *et al.*, 1996; Hardingham *et al.*, 2001), it is probable that HFS induced the activation of CREB through L-type VDCC alone (in the presence of CPP) and thereby increased the STX transcription level. Entry of calcium in this way is also likely to activate post-translational regulatory pathways such as, for instance, the activation of the protein kinase C (PKC), which has been shown to regulate the polysialyltransferases activity in chick ciliary ganglion (Bruses *et al.*, 1995; Bruses and Rutishauser, 1998). The question of whether the polysialization of NCAM is triggered solely through the activation of VDCC channels in normal conditions, or also via the activation of NMDA receptors when they are available remains to be tested.

Our result is compatible with the study of Stoenica and collaborators (2006) showing that *in vivo* plasticity in the DG of mice lacking PST or STX is intact, as they both suggest that, at least in DG, NCAM polysialylation may not be necessary for homosynaptic LTP. However, further experiments would be needed in order to test whether the increase and redistribution of PSA moieties is a mandatory process for HFS-induced synaptic plasticity in the DG. The most direct way, although not the easiest would, for example, be to test whether locally applied Endo-N treatment blocks homosynaptic LTP and

heterosynaptic LTD induction and their PSA-NCAM correlates in the DG *in vivo*.

The use of gold immunolabelling and EM allowed us to refine our analysis by quantifying where the PSA moieties were transported following synthesis. To our knowledge few studies have described the ultrastructural distribution of PSA-NCAM immunoreactivity in the DG. A couple of studies of the rat DG (Schuster *et al.*, 2001; Fux *et al.*, 2003) and an examination of the human DG (Mikkonen *et al.*, 1999) found, as in our study, that PSA moieties were primarily located on dendritic shaft and spines. Our EM analysis revealed mainly that the density of PSA positive dendrites diminishes in the MML following HFS of the LPP (heterosynaptic LTD) and that the PSA positive spine density is augmented as a result of MPP tetanization (homosynaptic LTP). It is therefore conceivable that, subsequent to synthesis in the cell body, PSA-NCAM is transported in the dendrites and inserted in activated spines; tetanization of the MPP would have then resulted in an increased spine density in the MML, and HFS applied to the LPP would have had the same effect but in the outer molecular layer (where LPP makes synapses), producing as a consequence a decrease in immunopositive dendrites in the MML. In other words, we propose that a strong activation of the granule cells up-regulates PSA-NCAM synthesis, which would then be incorporated into activated synapses. Future studies examining the colocalization of calcium staining with PSA-NCAM immunoreactivity would be necessary to test directly this hypothesis. It might seem puzzling that no increase in the density of PSA positive dendrites was observed after homosynaptic LTP in the MML, but this is possibly due to the proximity of this dendritic region with the granule cell bodies, responsible for a high level of PSA moieties at the basal level. The fact that the differences in PSA-NCAM immunolabelling were found mainly in dendrites and spines, as opposed to presynaptic boutons (despite a trend for a change in sub-cellular distribution both after homosynaptic LTP and heterosynaptic LTD), is consistent with data obtained in hippocampal heterogenotypic culture showing that synaptic coverage of neurons from NCAM deficient mice is markedly reduced relative to those from WT mice, thus suggesting that post-synaptic but not presynaptic NCAM is crucial for synapse stabilization (Dityatev *et al.*, 2000).

The alterations observed at the EM level were notably found to be NMDA-receptor independent, indicating that, akin to the increased PSA-NCAM synthesis, the redistribution of PSA moieties following HFS also depends on mechanisms not shared with homosynaptic LTP or heterosynaptic LTD. In a morphological investigation of dendritic and synaptic structure using three-dimensional ultrastructural analysis of similarly prepared tissue we found that homosynaptic LTP-induced alterations of the spine shape and, interestingly, that CPP impaired most but not all of these ultrastructural changes (unpublished data). Such a finding is consistent with an up-regulation of PSA synthesis and changes in subcellular distribution that may not solely be triggered by activation of the NMDA-receptors.

In summary, the present data support the view that polysialylation of the NCAM molecule is triggered by calcium entry resulting from strong synaptic activation and that this takes place in parallel to mechanisms underlying homosynaptic LTP. Although heterosynaptic LTD has recently been shown to require homosynaptic activity (Abraham *et al.*, 2007), we would like to note that the expression of PSA following homosynaptic LTD may differ from our present results in heterosynaptic LTD. In light of the data showing that PSA-NCAM increases in the DG following fear conditioning, odour discrimination or spatial learning (Fox *et al.*, 1995; Foley *et al.*, 2003; Venero *et al.*, 2006; Lopez-Fernandez *et al.*, 2007), and that impairing or promoting PSA-NCAM function accordingly affect learning (Florian *et al.*, 2006; Markram *et al.*, 2007), we raise the question of whether the increase in PSA observed after learning represents another form of plasticity which acts synergistically with LTP or LTD.

ACKNOWLEDGEMENTS

The authors wish to thank Gérard Dutrieux, Paulette Richer, Valérie Marsaux, Pascale Leblanc-Veyrac and Nathalie Samson for excellent technical assistance. This work is supported by the EU FPVI Promemoria programme (contract no. 512012).

Statement of interest

None.

Supplementary material

The supplementary material referred to in this article can be found online at journals.cambridge.org/ngb.

REFERENCES

Abraham W.C., Logan B., Wolff A. and Benuskova L. (2007) "Heterosynaptic" LTD in the dentate gyrus of anesthetized rat requires homosynaptic *activity*. *Journal of Neurophysiology* 98, 1048–1051.

Abraham W.C. and McNaughton N. (1984) Differences in synaptic transmission between medial and lateral components of the perforant path. *Brain Research* 303, 251–260.

Angata K. and Fukuda M. (2003) Polysialyltransferases: major players in polysialic acid synthesis on the neural cell adhesion molecule. *Biochimie* 85, 195–206.

Arami S., Jucker M., Schachner M. and Welzl H. (1996) The effect of continuous intraventricular infusion of L1 and NCAM antibodies on spatial learning in rats. *Behavioural Brain Research* 81, 81–87.

Becker C.G., Artola A., Gerardy-Schahn R., Becker T., Welzl H. and Schachner M. (1996) The polysialic acid modification of the neural cell adhesion molecule is involved in spatial learning and hippocampal long-term potentiation. *Journal of Neuroscience Research* 45, 143–152.

Bouzioukh F., Tell F., Jean A. and Rougon G. (2001) NMDA receptor and nitric oxide synthase activation regulate polysialylated neural cell adhesion molecule expression in adult brainstem synapses. *Journal of Neuroscience* 21, 4721–4730.

Bruses J.L., Oka S. and Rutishauser U. (1995) NCAM-associated polysialic acid on ciliary ganglion neurons is regulated by polysialytransferase levels and interaction with muscle. *Journal of Neuroscience* 15, 8310–8319.

Bruses J.L. and Rutishauser U. (1998) Regulation of neural cell adhesion molecule polysialylation: evidence for nontranscriptional control and sensitivity to an intracellular pool of calcium. *Journal of Cell Biology* 140, 1177–1186.

Chan J., Aoki C. and Pickel V.M. (1990) Optimization of differential immunogold-silver and peroxidase labelling with maintenance of ultrastructure in brain sections before plastic embedding. *Journal of Neuroscience Methods* 33, 113–127.

Deisseroth K., Bito H. and Tsien R.W. (1996) Signaling from synapse to nucleus: postsynaptic CREB phosphorylation during multiple forms of hippocampal synaptic plasticity. *Neuron* 16, 89–101.

Dityatev A., Dityateva G. and Schachner M. (2000) Synaptic strength as a function of post- versus presynaptic expression of the neural cell adhesion molecule NCAM. *Neuron* 26, 207–217.

Doyere V., Srebro B. and Laroche S. (1997) Heterosynaptic LTD and depotentiation in the medial perforant path of the dentate gyrus in the freely moving rat. *Journal of Neurophysiology* 77, 571–578.

Eckhardt M., Bukalo O., Chazal G., Wang L., Goridis C., Schachner M. *et al.* (2000) Mice deficient in the polysialyltransferase ST8SiaIV/PST-1 allow discrimination of the roles of neural cell adhesion molecule protein and polysialic acid in neural development and synaptic plasticity. *Journal of Neuroscience* 20, 5234–5244.

Eyre M.D., Richter-Levin G., Avital A. and Stewart M.G. (2003) Morphological changes in hippocampal dentate gyrus synapses following spatial learning in rats are transient. *European Journal of Neuroscience* 17, 1973–1980.

Florian C., Foltz J., Norreel J.C., Rougon G. and Roullet P. (2006) Post-training intrahippocampal injection of synthetic poly-alpha-2,8-sialic acid-neural cell adhesion molecule mimetic peptide improves spatial long-term performance in mice. *Learning & Memory* 13, 335–341.

Foley A.G., Hedigan K., Roullet P., Moricard Y., Murphy K.J., Sara S.J. *et al.* (2003) Consolidation of memory for odour-reward association requires transient polysialylation of the neural cell adhesion molecule in the rat hippocampal dentate gyrus. *Journal of Neuroscience Research* 74, 570–576.

Fox G.B., O'Connell A.W., Murphy K.J. and Regan C.M. (1995) Memory consolidation induces a transient and time-dependent increase in the frequency of neural cell adhesion molecule polysialylated cells in the adult rat hippocampus. *Journal of Neurochemistry* 65, 2796–2799.

Fux C.M., Krug M., Dityatev A., Schuster T. and Schachner M. (2003) NCAM180 and glutamate receptor subtypes in potentiated spine synapses: an immunogold electron microscopic study. *Molecular and Cellular Neurosciences* 24, 939–950.

Gascon E., Vutskits L. and Kiss J.Z. (2007) Polysialic acid-neural cell adhesion molecule in brain plasticity: from synapses to integration of new neurons. *Brain Research and Reviews* 56, 101–118.

Hammond M.S., Sims C., Parameshwaran K., Suppiramaniam V., Schachner M. and Dityatev A. (2006) Neural cell adhesion molecule-associated polysialic acid inhibits NR2B-containing N-methyl-D-aspartate receptors and prevents glutamate-induced cell death. *Journal of Biological Chemistry* 281, 34859–34869.

Hardingham G.E., Arnold F.J. and Bading H. (2001) Nuclear calcium signaling controls CREB-mediated gene expression triggered by synaptic activity. *Nature Neuroscience* 4, 261–267.

Hsu S.M., Raine L. and Fanger H. (1981) The use of antiavidin antibody and avidin-biotin-peroxidase complex in immunoperoxidase technics. *American Journal of Clinical Pathology* 75, 816–821.

Kiss J.Z. and Muller D. (2001) Contribution of the neural cell adhesion molecule to neuronal and synaptic plasticity. *Reviews in the Neurosciences* 12, 297–310.

Lopez-Fernandez M.A., Montaron M.F., Varea E., Rougon G., Venero C., Abrous D.N. *et al.* (2007) Upregulation of polysialylated neural cell adhesion molecule in the dorsal hippocampus after contextual fear conditioning is involved in long-term memory formation. *Journal of Neuroscience* 27, 4552–4561.

Markram K., Gerardy-Schahn R. and Sandi C. (2007) Selective learning and memory impairments in mice deficient for polysialylated NCAM in adulthood. *Neuroscience* 144, 788–796.

Mezey S., Doyere V., De Souza I., Harrison E., Cambon K., Kendal C.E. *et al.* (2004) Long-term synaptic morphometry changes after induction of long-term potentiation and long-term depression in the dentate gyrus of awake rats are not simply mirror phenomena. *European Journal of Neuroscience* 19, 2310–2318.

Mikkonen M., Soininen H., Tapiola T., Alafuzoff I. and Miettinen R. (1999) Hippocampal plasticity in Alzheimer's disease: changes in highly polysialylated NCAM immunoreactivity in the hippocampal formation. *European Journal of Neuroscience* 11, 1754–1764.

Mileusnic R., Lancashire C. and Rose S.P. (1999) Sequence-specific impairment of memory formation by NCAM antisense oligonucleotides. *Learning & Memory* 6, 120–127.

Miranda R., Blanco E., Begega A., Santin L.J. and Arias J.L. (2006) Reversible changes in hippocampal CA1 synapses associated with water maze training in rats. *Synapse* 59, 177–181.

Muller D., Wang C., Skibo G., Toni N., Cremer H., Calaora V. *et al.* (1996) PSA-NCAM is required for activity-induced synaptic plasticity. *Neuron* 17, 413–422.

Nacher J., Blasco-Ibanez J.M. and McEwen B.S. (2002) Non-granule PSA-NCAM immunoreactive neurons in the rat hippocampus. *Brain Research* 930, 1–11.

Nacher J., Rosell D.R., Alonso-Llosa G. and McEwen B.S. (2001) NMDA receptor antagonist treatment induces a long-lasting increase in the number of proliferating cells, PSA-NCAM-immunoreactive granule neurons and radial glia in the adult rat dentate gyrus. *European Journal of Neuroscience* 13, 512–520.

Nakagawa S., Kim J.E., Lee R., Chen J., Fujioka T., Malberg J. *et al.* (2002) Localization of phosphorylated cAMP response element-binding protein in immature neurons of adult hippocampus. *Journal of Neuroscience* 22, 9868–9876.

Nixon K., Kim D.H., Potts E.N., He J. and Crews F.T. (2008) Distinct cell proliferation events during abstinence after alcohol dependence: microglia proliferation precedes neurogenesis. *Neurobiology of Disease* 31, 218–229.

Paxinos G. and Watson C. (1998) *The Rat Nervous System*. New York: Academic Press, Spiral Bound.

Peters A., Palay S.L. and Webster H.D. (1991) *The Fine Structure of the Nervous System*. 3rd ed. New York: Oxford University Press.

Pickel V.M., Johnson E., Carson M. and Chan J. (1992) Ultrastructure of spared dopamine terminals in caudate-putamen nuclei of adult rats neonatally treated with intranigral 6-hydroxydopamine. *Developmental Brain Research* 70, 75–86.

Platano D., Fattoretti P., Balietti M., Giorgetti B., Casoli T., Di Stefano G. *et al.* (2008) Synaptic remodeling in hippocampal CA1 region of aged rats correlates with better memory performance in passive avoidance test. *Rejuvenation Research* 11, 341–348.

Reynolds E.S. (1963) The use of lead citrate at high pH as an electron-opaque stain in electron microscopy. *Journal of Cell Biology* 17, 208.

Rougon G. (1993) Structure, metabolism and cell biology of polysialic acids. *European Journal of Cell Biology* 61, 197–207.

Roullet P., Mileusnic R., Rose S.P. and Sara S.J. (1997) Neural cell adhesion molecules play a role in rat memory formation in appetitive as well as aversive tasks. *Neuroreport* 8, 1907–1911.

Rutishauser U. (2008) Polysialic acid in the plasticity of the developing and adult vertebrate nervous system. *Nature Reviews. Neuroscience* 9, 26–35.

Rutishauser U. and Landmesser L. (1996) Polysialic acid in the vertebrate nervous system: a promoter of plasticity in cell-cell interactions. *Trends in Neurosciences* 19, 422–427.

Schachner M. (1997) Neural recognition molecules and synaptic plasticity. *Current Opinion in Cell Biology* 9, 627–634.

Schuster T., Krug M., Hassan H. and Schachner M. (1998) Increase in proportion of hippocampal spine synapses expressing neural cell adhesion molecule NCAM180 following long-term potentation. *Journal of Neurobiology* 37, 359–372.

Schuster T., Krug M., Stalder M., Hackel N., Gerardy-Schahn R. and Schachner M. (2001) Immunoelectron microscopic localization of the neural recognition molecules L1, NCAM, and its isoform NCAM180, the NCAM-associated polysialic acid, beta1 integrin and the extracellular matrix molecule tenascin-R in synapses of the adult rat hippocampus. *Journal of Neurobiology* 49, 142–158.

Seki T. and Arai Y. (1993) Distribution and possible roles of the highly polysialylated neural cell adhesion molecule (NCAM-H) in the developing and adult central nervous system. *Neuroscience Research* 17, 265–290.

Sheng M., Thompson M.A. and Greenberg M.E. (1991) CREB: a Ca(2+)-regulated transcription factor phosphorylated by calmodulin-dependent kinases. *Science* 252, 1427–1430.

Singh J. and Kaur G. (2007) Transcriptional regulation of polysialylated neural cell adhesion molecule expression by NMDA receptor activation in retinoic acid-differentiated SH-SY5Y neuroblastoma cultures. *Brain Research* 1154, 8–21.

Stewart M.G., Medvedev N.I., Popov V.I., Schoepfer R., Davies H.A., Murphy K. *et al.* (2005) Chemically induced long-term potentiation increases the number of perforated and complex postsynaptic densities but does not alter dendritic spine volume in CA1 of adult mouse hippocampal slices. *European Journal of Neuroscience* 21, 3368–3378.

Stoenica L., Senkov O., Gerardy-Schahn R., Weinhold B., Schachner M. and Dityatev A. (2006) In vivo synaptic plasticity in the dentate gyrus of mice deficient in the neural cell adhesion molecule NCAM or its polysialic acid. *European Journal of Neuroscience* 23, 2255–2264.

Vaithianathan T., Matthias K., Bahr B., Schachner M., Suppiramaniam V., Dityatev A. *et al.* (2004) Neural cell adhesion molecule-associated polysialic acid potentiates alpha-amino-3-hydroxy-5-methylisoxazole-4-propionic acid receptor currents. *Journal of Biological Chemistry* 279, 47975–47984.

Venero C., Herrero A.I., Touyarot K., Cambon K., Lopez-Fernandez M.A., Berezin V. *et al.* (2006) Hippocampal up-regulation of NCAM expression and polysialylation plays a key role on spatial memory. *European Journal of Neuroscience* 23, 1585–1595.

Wang C., Pralong W.F., Schulz M.F., Rougon G., Aubry J.M., Pagliusi S. *et al.* (1996) Functional N-methyl-D-aspartate receptors in O-2A glial precursor cells: a critical role in regulating polysialic acid-neural cell adhesion molecule expression and cell migration. *Journal of Cell Biology* 135, 1565–1581.

AUTHORS' ADDRESSES

[1] Faculty of Life Sciences
The University of Manchester
Manchester, UK

[2] Institute of Experimental Medicine
ASCR
Prague, Czech Republic

[3] NAMC
CNRS-UMR8620
Université Paris-Sud
Orsay, France

[4] Department of Life Sciences
The Open University
Milton Keynes, UK

Correspondence should be addressed to:
V. Doyère
CNRS-UMR8620, NAMC
Université Paris-Sud, Bat. 446
91405 Orsay, France
phone: +33 (0)169 154 987
email: valerie.doyere@u-psud.fr
J. J. Rodríguez
Faculty of Life Sciences
The University of Manchester
AV Hill Building
Room 2.002, Oxford Road
Manchester M13 9PT, UK
phone: +44 (0)161 275 7324
email: Jose.Rodriguez-arellano@manchester.ac.uk